Structural Health Monitoring Data Transmission for Composite Hydrokinetic Turbine Blades

A. Heckman[1], J. L. Rovey[2], K. Chandrashekhara[3], S. E. Watkins[4], D. S. Stutts[5], A. Banerjee[6], R. S. Mishra[7]

[1, 2, 3, 5]Mechanical and Aerospace Engineering, Missouri University of Science and Technology, Rolla, Missouri, 65409, USA

[4]Electrical and Computer Engineering, Missouri University of Science and Technology, Rolla, Missouri, 65409, USA

[6]Mechanical Engineering and Mechanics, Lehigh University, Bethlehem, Pennsylvania,18015 USA

[7]Materials Science and Engineering, University of North Texas, Denton, Texas, 76203, USA

[1] ajhr4c@mst.edu; [2] roveyj@mst.edu; [3]chandra@mst.edu; [5] stutts@mst.edu; [4] watkins@mst.edu; [6]arb612@lehigh.edu; [7]rajiv.mishra@unt.edu

Abstract- **A health monitoring approach is investigated for hydrokinetic turbine blades. In-service monitoring is critical due to the difficult environment for blade inspection and the cost of inspection downtime. Composite blade designs provide a medium for embedding sensors into the blades for in-situ health monitoring. The major challenge with in-situ health monitoring is transmission of sensor signals from the remote rotating reference frame of the blade to the system monitoring station. In the presented work, a novel system for relaying in-situ blade health measurements in hydrokinetic systems is described and demonstrated. An ultrasonic communication system is used to transmit sensor data underwater from the rotating frame of the blade to a fixed relay station. Data are then broadcast via radio waves to a remote monitoring station. Results indicate that the assembled system can transmit simulated sensor data with an accuracy of ±5% at a maximum sampling rate of 500 samples/sec. A power investigation of the transmitter within the blade shows that continuous max-sampling operation is only possible for short durations (~days), and is limited due to the capacity of the battery power source. However, intermittent sampling, with long periods between samples, allows for the system to last for very long durations (~years). Finally, because the data transmission system can operate at a high sampling rate for short durations or at a lower sampling rate/higher duty cycle for long durations, it is well-suited for short-term prototype and environmental testing, as well as long-term commercially-deployed hydrokinetic machines.**

Keywords- Marine Energy; Hydrokinetic Energy; Structural Health Monitoring; Acoustic Communication

I. INTRODUCTION

Hydrokinetic energy systems are designed to convert kinetic energy of a fluid (e.g., river or tidal current, or waves) into electricity [1-2]. In a typical rotating device, the river or tidal current passes through a protection screen and into the turbine channel. Kinetic energy of the fluid causes the turbine to rotate and this rotational energy is converted to electrical energy with a generator attached at the top of the turbine. Many hydrokinetic energy systems plan to be located off-shore or in remote areas far from dense population. For example, a study of potential Alaska river in-stream power plants selected three river locations where the nearest villages have populations of 50-100 people and the nearest cities are 100 s of miles away [3]. Simply getting to these sites represents a significant challenge. Accessing the components to perform any kind of analysis would be a difficult, expensive, and a nearly impossible task. Hydrokinetic energy systems must be remotely monitored.

The main benefit of remote monitoring is lower O&M costs and a higher return on investment. The Pew Center on Global Climate Change recently found that "O&M costs could remain high due to difficult access and working conditions unless machines are developed that can be unattended for long periods of time" [4]. It is difficult to estimate the future O&M costs of hydrokinetic systems because the technology is still being developed. However, wind energy systems are plagued by similar issues and, over the lifetime of a machine, have typical O&M costs of 70-95% of the total investment cost [5]. These data are from a project that considered six hundred 750 kW wind turbines. O&M costs are typically higher for smaller power machines and near-term hydrokinetic systems are likely to be a few 100 kW, in which case O&M costs may be higher. Reducing O&M costs with remote monitoring is imperative for making these systems viable for widespread use.

The structural health of hydrokinetic energy systems needs to be monitored. While methods for remotely monitoring hydrokinetic system parameters such as voltage and power output have been developed, the ability to monitor the structure, specifically the turbine blades, has yet to be developed. Monitoring the turbine blade is essential as it is the critical component for energy extraction and as such it also bears the most dynamic load. Fatigue causes degradation of structures and eventually leads to structure failure. In addition to the natural slow fatigue of the blade structure, there is also significant concern about transient impacts and loads due to environmental factors. Oceans and rivers are heterogeneous bodies of water that contain aquatic and marine organisms, vegetation due to run-off, and pollution that pose a significant hazard to hydrokinetic energy systems. Multiple reports have been published evaluating the effect of hydrokinetic energy systems on marine life (e.g., fish and other aquatic organisms, diving birds, and mammals) [6-9]. While a single impact may not be immediately catastrophic, it can create a crack at the point of impact that eventually propagates, compromising the structural integrity of the blade and leading to failure. In addition, other transient environmental effects may cause increased loads on the blade, degrading

structural integrity. For example, earthquakes, tsunamis, and flooding are all natural phenomena that will occur and may cause damage.

There are multiple scenarios where remote monitoring of turbine blade structural health is beneficial. For example, (1) it can lead to timely replacement of a blade by notifying service personnel when the blade structural integrity is likely to fail; (2) in the event of damage due to transient environmental effects, the remote monitor would immediately notify service personnel so the system could be repaired quickly to minimize down-time; (3) knowledge of the turbine blade structural health could lead to enhanced operational lifetime. For example, as the blades age, the system may be operated at reduced capacity to reduce structural load, thereby maintaining power generation (albeit at a reduced level) for a longer period of time.

The challenge with in-service monitoring the structural health of any turbine blade is that it is a rotating component that is always moving when the system is operating. So connecting a wire to a fiber optic, acoustic sensor, electrical strain gage, etc. is not practical. This challenge can be overcome by wirelessly transmitting data from the rotating frame of the blade. Wireless structural health data obtained via acoustic monitoring were successfully transmitted from a wind turbine blade [10-12]. But simply adapting this wind turbine system to a hydrokinetic turbine blade is not advisable since sea water severely attenuates electromagnetic signals and as such limits transmission frequencies to 30-300 Hz and requires large antennas and high transmission power [13].

Structural health monitoring of hydrokinetic turbine blades has not been investigated to the authors' knowledge and is the focus of the work presented here. In the following sections we describe proof-of-principle laboratory experiments that demonstrate transmission of a simulated structural health monitoring signal through the aquatic environment and then wirelessly through air to a remote monitoring station. A schematic of the general concept is shown in Fig. 1. Composite turbine blades, embedded with a fiber optic strain gage and acoustic transducer, are attached to the turbine and used to generate electricity. The fiber optic strain gage senses the strain of the blade structure over time due to cyclic loading (fatigue) and transient environmental factors. A power and electronics module inside the blade conditions the fiber optic strain gage signal into an acoustic signal that is transmitted by the acoustic transducer. The acoustic waves propagate through the water to a receiver that is located near the shore or on the system foundation. The received acoustic signal is then broadcast above water long distances by radio waves to the monitoring station. The broadcast signal is then interpreted at the monitoring station, yielding strain data from the blade, which can be used to notify service and maintenance personnel.

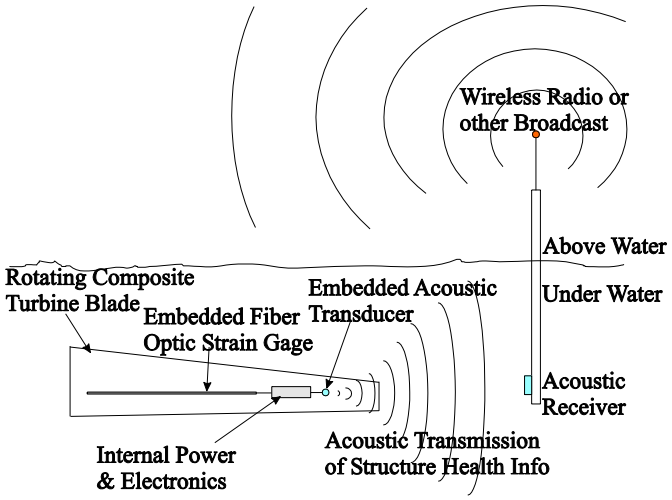

Fig. 1 Schematic of the hydrokinetic turbine blade structural health monitoring concept

In the following sections we describe our proof-of-concept demonstration of the data transmission part of the blade structural health monitoring concept. We have demonstrated our ability to manufacture an instrumented turbine blade in Refs. [14] and [15]. In the following study, a simulated strain gage output was used as the input to the data transmission system. The system was demonstrated in both a bench top environment and on a prototype hydrokinetic turbine in a laboratory environment (water tunnel). In addition to demonstrating the feasibility of the technique, we also present results from a power analysis that is used to assess the viability of the approach and its suitability for both commercial and prototype hydrokinetic energy systems. We envision this novel concept and the resulting capability to enable blade structural health monitoring in both long-term commercial hydrokinetic system deployment, as well as in prototype environmental impact studies.

II. DATA TRANSMISSION PROCESS AND SYSTEM

A schematic of the data transfer process is shown in Fig. 2. The system described here uses an acoustic communication system for underwater data transmission, while the above water (air) data transmission uses a wireless Bluetooth transmitter. As shown in Fig. 2, a 0-10 V source simulates the data output from a strain gage embedded in the turbine blade [14-15]. In an

integrated final system, the strain gage signal would be modulated and analyzed using embedded electronics that would output a voltage signal based on the measured strain. The actual voltage that would need to be transmitted would be dependent on the desired strain analysis and the embedded electronics. Here we have assumed that this signal would vary between 0-10 V, but the communication system could be modified to accommodate other input signal ranges. This simulated strain analysis signal is encoded by the transmitter electronics and acoustically transmitted through the water. The encoded data signal is received by an underwater microphone connected to the receiver electronics, which then decodes the signal and broadcast it wirelessly through air via Bluetooth. A remote computer with a Bluetooth receiver serves as the remote monitoring station.

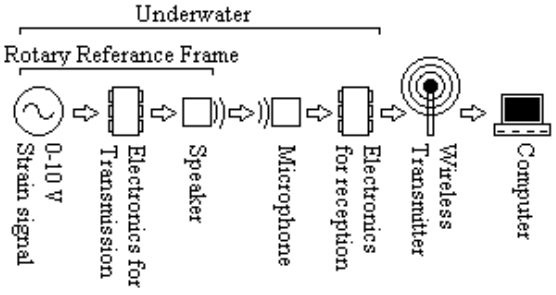

Fig. 2 Schematic of main components of the underwater acoustic communication system

A. Acoustic Transmitter and Receiver Circuitry

The acoustic transmitter and receiver circuits consist of two main components: a microcontroller and an ultrasonic transducer. The foundation of the transmission and reception circuitry are two PIC18F46K20 Microchip microcontrollers (MCUs), one for each circuit. These MCUs provide the necessary processing to encode and decode the data. A pair of MA40MF14-5B Murata ultrasonic transducers serve as the acoustic transmitter and receiver. These transducers are optimized for 40 kHz frequency, and were selected based on the rationale described below.

The main tasks of the transmitter circuit are to measure the strain sensor voltage, measure the battery voltage, enter and awake from "sleep" mode, encode the strain data into an acoustic signal, and transmit the data with the ultrasonic transducer. A schematic of the transmitter circuit is shown in Fig. 3. Measuring the sensor voltage and battery voltage is done using the MCUs built-in ADC feature. Measuring the battery voltage allows us to also track the life of the power supply. The voltage divider at the strain sensor is used to lower the 0 to 10 V simulated strain gage signal to 0 to 2 V, since the MCU input pins can only take 0 to 5 V. The effect of duty cycle on the potential lifetime of the monitoring system is studied in subsequent sections by using the "sleep" feature of the MCU, which is controlled using the MCU software. MCU software is also used to encode the measured strain gage voltage into the acoustic transmission signal. Transmission of the acoustic signal uses the 40 kHz ultrasonic transducer, a DC to DC converter, and a logic level MOSFET. While initial tests showed that the MCU alone can drive the transducer, the resulting ultrasonic signal was too weak to ensure accurate reception. Instead a simple amplification circuit is used. The MCU output operates the MOSFET switch, which in turn modulates the transducer driving signal from the DC to DC converter. Finally, a 3 V power supply is used to power the circuit. For much of the testing, the power source was a DAQ, as shown later in the bench top setup, but a 3 V, 24 mm coin cell battery was used during testing on the hydrokinetic machine.

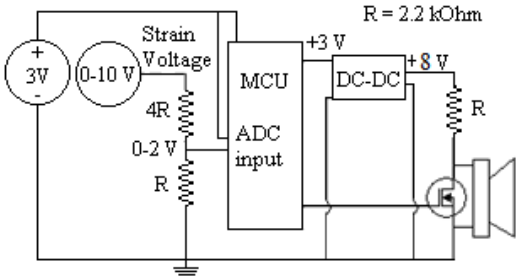

Fig. 3 Transmitter Circuit

The major tasks for the receiver circuit, shown in Fig. 4, are to receive the acoustic signal, process it, and re-transmit wirelessly through air (Bluetooth in this case). An ultrasonic transducer receives the transmitted acoustic signal. First, the signal passes through a charge amplifier which converts the charge developed across the piezoelectric transducer into a voltage proportional to the gain of the amplifier. The signal is then passed through an active high pass filter with a cutoff frequency of approximately 32 kHz and a gain value of 667, thus filtering and further amplifying the received signal. The filtering process allows the required 40 kHz signal through while removing anticipated background noise that would be found in a river, such as rain, wind, and fish acoustics. After being filtered and amplified, the signal is then modified by two comparators in sequence. The comparators convert the roughly sinusoidal signal into a clean square wave pulse train, which is easier for the MCU to process.

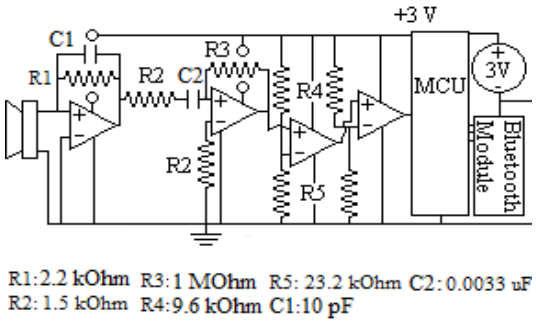

Fig. 4 Receiver Circuit

B. Acoustic Transmission Frequency

A 40 kHz acoustic signal was selected based on three main considerations. First, ambient noise sources encountered in the hydrokinetic energy system environment, both natural and artificial, were considered. Two natural sources and two artificial sources of ambient noise are likely to be encountered underwater in a river. The two natural sources are wind and rain noise, and aquatic animals, while the artificial noise sources originate from boat motors and ultrasonic range/fish finders. Both wind and rain have distinct acoustic power spectrums [16]. Wind noise can be approximated using Knudsen curves, which show that at about 500 to 1000 Hz, the magnitude of wind noise decreases with increasing frequency. While the wind noise does not disappear entirely in the ultrasonic region, it is severely reduced in strength and is not considered a significant noise source. Rain has a distinct peak in strength at around 14 to 16 kHz [16], and then also decreases in strength with increasing frequency. However, rain has been shown to suppress wind noise, and its peak is closer to the ultrasonic range. As such, of the two natural sound sources rain is the more concerning. For artificial noise sources, motor boat noise does not exceed 1 kHz [17], and therefore is not a concern for the ultrasonic frequencies used here. However, the commercial sonar products that many boats are equipped with are a concern, as they rely on producing ultrasonic pings to visualize the underwater environment. The frequency for commercial sonar applications ranges from 20 kHz to 400 kHz generally, and the most common frequencies used are 50 kHz and 200 kHz. Therefore selecting an ultrasonic communication frequency away from 50 or 200 kHz is best for mitigating interference from such ultrasonic devices.

The second criterion we evaluated was the audibility of the communication signal to humans. Specifically, we require the operating frequency to be inaudible to the human ear. This criterion is selected to reduce noise pollution that would potentially be generated by the system operation, and as such it is highly desirable that the signal produced be inaudible to both humans and many aquatic river organisms. The selection of an ultrasonic frequency is an easy way to alleviate this concern, as humans cannot hear in the ultrasonic range and many fish species can only hear in a range of 20 to 300 Hz [17].

The third criterion considered was signal attenuation and transmission rate in an underwater environment. In acoustic communication in water, the rate of attenuation and maximum data transmission rate are directly linked. More specifically, as frequency increases both the attenuation rate and the data transmission rate increase. Thus, a very low frequency signal can travel very large distances in water, but has a very slow rate of data transmission, whereas a high frequency ultrasonic signal travels shorter distances, but has higher data transmission rate. The attenuation of acoustic waves in seawater is shown in Fig. 5 and is given by Ainslie and McColm [18] as

$$\alpha = 0.00049 f^2 \exp(-(T/27 + D/17)) \tag{1}$$

where f is the frequency in kHz, T is temperature in degrees Celsius, and D is depth underwater in kilometers. Fig. 5 assumes a temperature of 22 ℃ and depth of 1 m, which is representative of a hydrokinetic system environment.

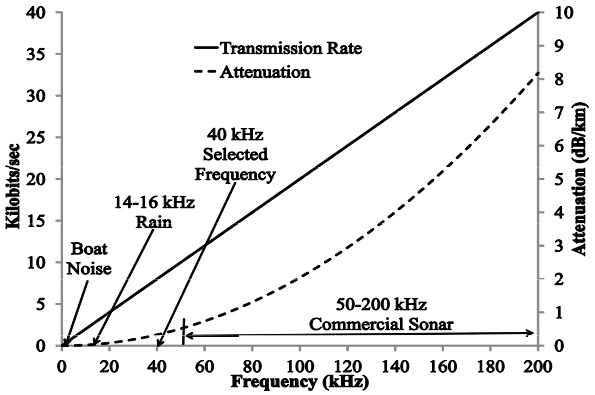

Fig. 5 Attenuation and transmission rate of transmitter circuit vs. frequency in sea-water (22 ℃) at depths of 1 m

The transmission rate is simply the frequency of the waveform divided by the number of periods that are used to represent one bit of data. The system described here uses 5 periods of the 40 kHz waveform to represent one bit and the resulting transmission rate is shown in Fig. 5. Since having both low attenuation rate and a high data transmission rate are mutually exclusive, the operating frequency for the system must be selected for the systems' requirements. We selected a 40 kHz signal because it has low attenuation rate on the order of 0.5 dB/km and relatively high 8 kbits/sec rate of data transfer. While higher frequency and the resulting higher data transfer rate would increase the "real-time" nature of the transmission, for this proof-of-concept system we place more emphasis on low attenuation so as to maintain a high signal-to-noise ratio and maintain reliable communication.

C. Data Encoding

The software running on the two MCUs encodes the structural health data for underwater transmission from the rotating blade and then decodes the data once received at the static relay station. In order to transmit the acquired data (simulated here as a voltage signal between 0-10 V), the transmitter MCU encodes the data before it is sent. This encoding for transmission is a modified on-off keying (OOK) encoding scheme, where a '1' data bit is indicated with 5 periods of the 40 kHz sine wave and a '0' data bit is indicated with a period of silence that lasts the equivalent time of 5 periods of the 40 kHz sine wave (i.e., 125 μs). Fig. 6 illustrates the encoding scheme. We have modified the standard OOK encoding by including four clock train '1' bits at the beginning of the data transmission sequence and also padding the space between each clock-train bit in the transmission with a period of silence. This modification eliminates the effect of echo encountered in the underwater environment. The four clock bits allow the receiving circuit to synchronize with the transmitting circuit, thus preventing the receiving circuit from triggering on an erroneous echo signal.

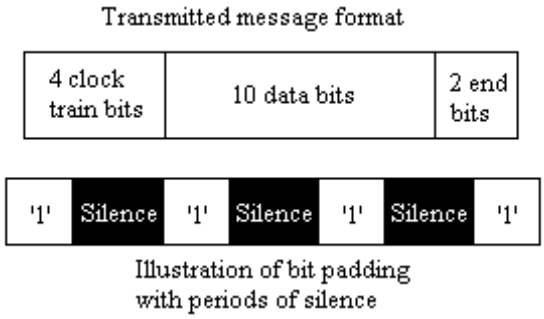

Fig. 6 Signal encoding scheme

The MCU of the receiver circuit listens for and receives transmissions, determines if the transmission is valid, decodes the transmission, and then rebroadcasts the data via Bluetooth. Since the receiving circuit is not in the rotary frame of reference, it can be powered directly from the turbine (or wall during lab testing) and therefore does not spend time sleeping like the transmitter. Instead it spends most of its time listening for an incoming transmission. Upon initial detection of a 40 kHz signal, the MCU determines if the signal is the 4-bit clock-train indicating initiation of data transmission by listening for the four '1' bits with silence in between (as illustrated in Fig. 6). The MCU then times the duration between each of the clock bits, and takes the average time of the periods of silence between them. In this way the MCU synchronizes with the transmitter. The next 10 data bits are then received as well as the two stop bits, which serve to indicate that the message has been successfully transmitted. If both stop bits are not received, the MCU rejects the data as not being a valid communication. In the case of correct transmission, the 10 data bits are converted back to a positive integer value and saved for retransmission via the Bluetooth. Once all the data packets from the transmitter have been received and saved, the saved data are then transmitted from the MCU to the attached Bluetooth module, which then relays the data wirelessly to a remote monitoring station. Following Bluetooth transmission, the receiver MCU returns to listening for the next communication.

D. Static Bench Top Testing

The electronics and software were tested to validate correct operation and to characterize the power use of the system. For these experiments a static bench top setup was used. For this setup only the acoustic transducers were placed in water, the other electronics are dry, and all components are statically mounted, i.e., there is no rotating turbine blade reference frame, only the lab frame. A photograph of the setup is shown in Fig. 7. In the figure, a NI USB-6008 DAQ (1) simulates a coin cell battery by providing a constant 3 V power supply to the various electric components. A Sparkfun BlueSMiRF Silver chip (2) is the Bluetooth transmitter connected to the receiver circuit (3). Both the receiver and transmitter circuits (4) are connected to an ultrasonic transducer in the aquatic environment (5). Finally, a Tektronix TDS-2014B oscilloscope (6) was used to measure voltage input and output from the various electric circuit components. To characterize the power of the transmitter circuit, the required current and time duration of the different modes of the MCU were measured. For the current measurement, a 3 V coin cell battery was used instead of the DAQ to insure the accuracy of the measurements. The current was measured with a Fluke multi-meter in series with the battery and circuit, while the time duration for each mode was measured with the oscilloscope.

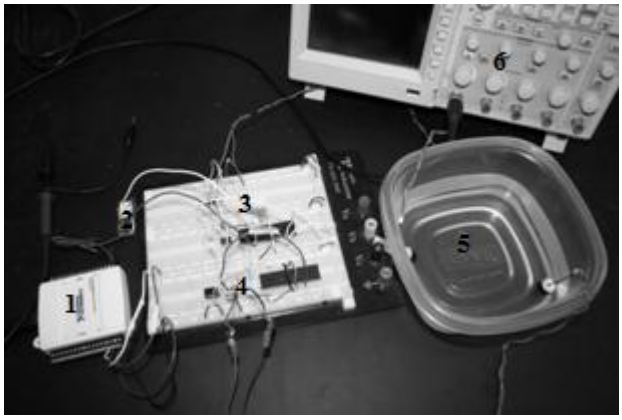

Fig. 7 Bench top setup for communication validation and power consumption investigation

E. Dynamic Hydrokinetic Testing Platform

The data transmission system was also tested on a hydrokinetic turbine in a water tunnel in order to better replicate the real world operating environment. A numerical investigation of this machine is presented in Ref. [19]. The water tunnel is capable of laminar flow up to 1 m/s (1.9 kts) and has a test section cross-section of 38.1x50.8 cm and length of 152.4 cm. For tests presented here, the water flow speed was 0.25 m/s and the hydrokinetic turbine had a rotational speed of around 42 rpm. The hydrokinetic turbine has a shaft diameter of 0.94 cm and is made of aluminum. The turbine has three constant chord blades that are made of aluminum with a blade width of 1.27 cm and blade length of 12.7 cm.

The data transmission system was mounted to the hydrokinetic machine and water tunnel as shown in Fig. 8. The receiver circuit was mounted on top of the tunnel (dry), with the receiving transducer located in the water and approximately 7.5 cm directly upstream of the transmitter along the centerline axis of the turbine shaft. The receiving transducer was oriented to collect acoustic signals travelling in the upstream direction from the hub. The transmitting circuitry and transducer were attached to the rotating frame of the hydrokinetic machine underwater. The transducer was mounted to the nose of the turbine hub on the centerline axis of the shaft and oriented to transmit data in the upstream direction. The transmitter circuitry was encased in a waterproof container attached to the turbine shaft.

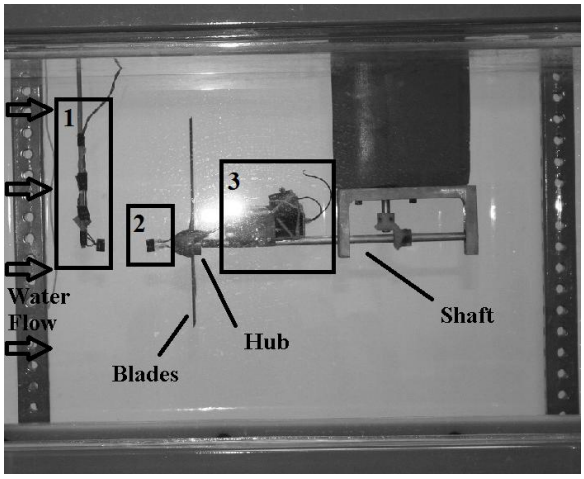

Fig. 8 Water Tunnel Test Section with (1) Receiver Transducer, (2) Transmitting Transducer, and (3) Power and Electronics Module

III. RESULTS AND DISCUSSION

First we describe the initial validation process that demonstrates accurate transmission of simulated structural health data from the blade to the remote monitoring station. This process is demonstrated for multiple simulated health data signals. Then we analyze the power requirements of the system and investigate the effect of operation mode on transmitter power supply lifetime. Finally, we demonstrate the technique in a dynamic environment by attaching the data communication system to a prototype hydrokinetic turbine in a water tunnel.

A. Data Transmission Validation

To demonstrate and validate the data communication process, several different health data waveforms were communicated. These different waveforms simulate possible outputs from the embedded fiber optic strain gauge. For the results presented

below, the communication system is tested in a static benchtop environment.

The ADC of the MCU has a resolution of 10 bits. This corresponds to 1023 separate voltage values that can be measured in the range from 0 V to the saturation voltage of the ADC, which is either 5 V or the voltage supplied to the MCU. In this case, the MCU supply voltage is 3 V, meaning that the theoretical precision of the ADC is 2.9 mV. To experimentally determine the accuracy of the ADC and associated transmission circuitry, we applied known voltages to the voltage divider and measured the resulting received signal from the monitoring station. Specifically, voltages from 1.2 to 3.0 V were applied with a resulting experimentally determined error of ±5%. So the 10-bit resolution provides a precision of 2.9 mV with an error in the reported data of ±5%.

Received data for the constant value and square wave waveforms are shown in Fig. 9. For the constant value data transmission, a voltage of 0.499±0.005 V was input into the transmitter circuit. As Fig. 9 shows, the remote monitoring station received 50 data points over a time period of 6.2 seconds, all of which have a value of 0.495±0.025 V. For the square wave, the period of the wave was chosen as 10 data samples with a min and max voltage of 0.367±0.005 V and 0.733±0.005 V, respectively. The waveform was connected to the transmitter circuit and the remote monitoring station received the signal shown in Fig. 9, with all output voltages within ±5% of the input.

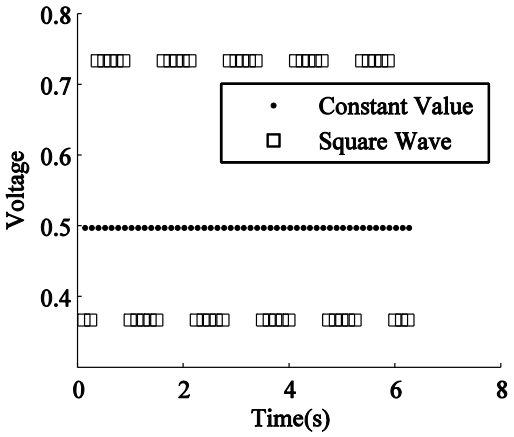

Fig. 9 Constant and square wave simulated structural health data transmitted to the remote monitoring station

Results from the half-cycle of a sine wave data transmission are shown in Fig. 10, along with the input signal. A slowly varying 0.08 Hz sine wave with an amplitude of 4.70±0.01 V was the input. Over the 6.2 second long half-cycle, the communication system transmitted 50 data points corresponding to discretized points of the sine wave. The received data are within the previously measured ±5% of the measured input voltage.

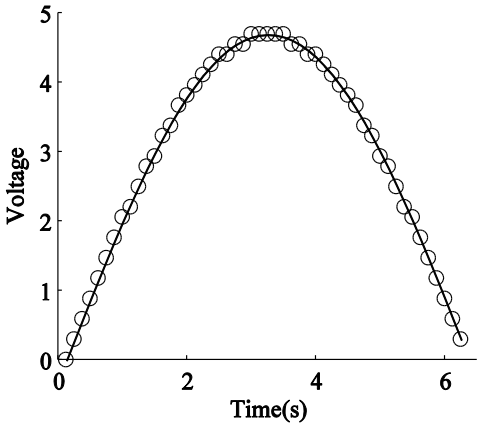

Fig. 10 Half-cycle sine wave simulated structural health data transmitted to the remote monitoring station

Finally, we assessed the fraction of transmitted data points that result in an error output from the receiver circuit, and we call this the data error fraction. The system was setup to act as it would in actual operation, transmitting a set of data (simulated in this case), sleeping, then transmitting more data. Over the course of four iterations of this procedure, consisting of 4400 data points, we found that 0.1% of the transmitted data points were in error.

B. Testing on a Dynamic Hydrokinetic Energy Platform

The data transmission system was setup and operated on a dynamic hydrokinetic energy platform that was described in Section III.E. The data transmission was programmed to be exactly the same as described in Section IV.A. Identical results

were obtained as shown in Fig. 9 and Fig. 10. In other words, data received by the remote monitoring station during dynamic testing on the hydrokinetic machine were identical to that shown in Fig. 9 and Fig. 10. This result indicates that the data transmission system can be operated in a relevant environment and within the rotating reference frame of the hydrokinetic blades. However, initially we find that more of the transmitted data results in an error from the receiver circuitry. While the benchtop setup had a data error fraction of 0.1%, we find that when testing on the hydrokinetic machine about 2% of the data points result in an error output from the receiver.

The increase in data error fraction during the initial test is due to the larger aquatic environment and the resulting increase in expansion and attenuation of the acoustic signal. We modified the setup shown in Fig. 8 by placing a 7.62-cm-diameter by 11.43-cm-long cylinder between the transmitting and receiving transducers. The cylinder was attached to the receiver and was therefore statically mounted (not rotating). The cylinder reduces the expansion and attenuation of the acoustic signal by guiding the acoustic waves from the transmitter to the receiver. With this modified setup, we find that only 0.9% of the data result in an error output.

C. Power Analysis

The power requirements of the transmitter circuit were investigated in order to assess and predict the operational lifetime of the communication system. We envision the transmitter circuit embedded into the hub of the turbine shaft and battery powered within the rotating reference frame of the turbine. While other power options are available, including energy harvesting and a shaft-mounted power take-off, the following analysis assumes the transmitter is operated with a battery of known capacity. The receiver circuit is statically located and can be fed power directly from the generator, so its power consumption is not limited and not investigated here.

Power consumption is calculated using the measured voltage and current output by the battery of the transmitter circuit. In this case, the battery is outputting a constant 3 V signal. The static bench top setup was used with the exception that the battery was used to power the transmitter circuit. Current drawn from the battery was measured for the three possible modes of transmitter circuit operation: sleep, sampling, and transmission. The time the transmitter spends in each of these modes is also measured. These results are given in Table I. The ‘X’ used in Table I is called the duty cycle, the ratio of time spent ‘asleep’ to time ‘awake’. A plot of the current consumption of the transmitter as a function of duty cycle is shown in Fig. 11.

TABLE I TRANSMITTER CURRENT DURING DIFFERENT OPERATING MODES (3 V BATTERY SUPPLY)

Mode	Time (ms)	Current (mA)	Current*Time(mA*ms)
Sleep	160.1X	0.03	4.80X
ADC sampling	0.1	2.31	0.23
Transmission	160	10.01	1601.6

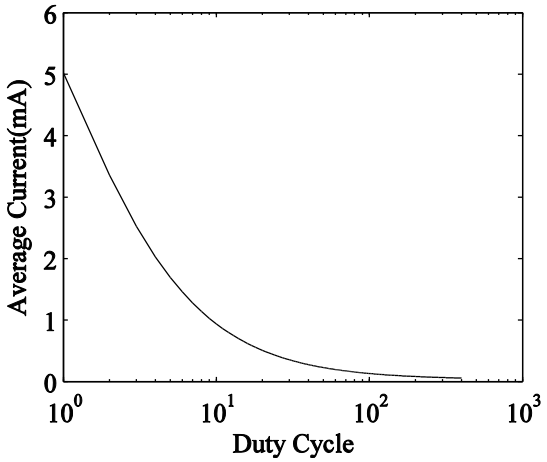

Fig. 11 Time averaged current draw of the transmitter circuit vs. duty cycle (ratio of time spent ‘asleep’ to time ‘awake’)

The maximum operational duration of the transmitter can be estimated using the average current data and known battery capacity. Battery capacity (measured in mA-hr) is divided by the average current, yielding the maximum time in hours that the battery can source the required current. Using the average current results from Fig. 11, the maximum operational lifetime of the transmitter circuit is plotted in Fig. 12 for batteries with different capacity. The battery capacities shown in Fig. 12 are typical of commercial off-the-shelf coin cell batteries. Table II highlights the duty cycle required to achieve a desired duration of operation, along with the time the transmitter spends sleeping for that duty cycle. For example, to power the transmitter for 1 year using a 560 mA-hr coin cell battery requires a duty cycle of 294, which means data will be acquired and transmitted about every 47 seconds for the entire year.

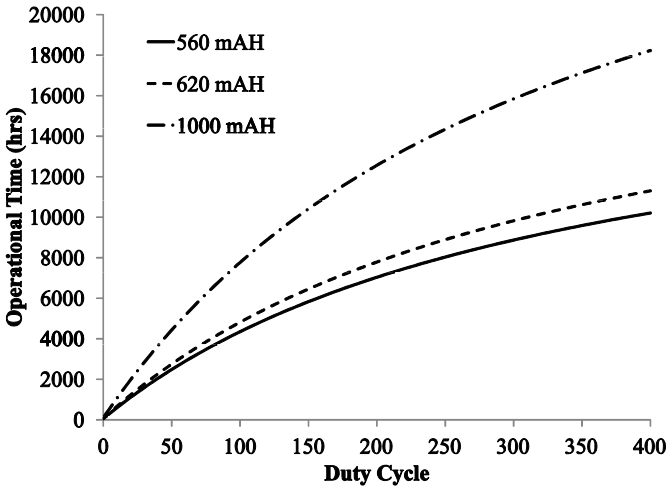

Fig. 12 Predicted transmitter circuit operating time vs. duty cycle for different battery capacity

TABLE II DUTY CYCLE AND SLEEP DURATION FOR A DESIRED TRANSMITTER CIRCUIT OPERATING TIME FOR VARIOUS BATTERY CAPACITIES

Operating Time	Duty Cycle ('Sleep' Time (sec))		
	560 mA-hr	620 mA-hr	1000 mA-hr
1 week	3 (0.48)	2 (0.32)	2 (0.32)
2 weeks	6 (0.96)	5 (0.80)	3 (0.48)
1 month	12 (1.92)	11 (1.76)	6 (0.96)
½ year	91 (14.57)	80 (12.81)	45 (7.20)
1 year	294 (47.07)	244 (39.06)	118 (18.89)
2 years	5080 (813)	1851 (296)	368 (58.92)

Results indicate that the data transmission system should be operated in different modes depending on the desired application. Specifically, the transmitter circuit should be operated with a duty cycle suited for the duration of the application. To achieve longer operational duration of the transmitter, a higher duty cycle is required. We anticipate that commercially deployed hydrokinetic machines will require long operational duration and thus high duty cycle, while shorter-term environment assessment studies will benefit from lower duty cycle operation. For example, environmental assessment testing of a prototype machine is a relatively short timeline on the order of days or weeks compared with a commerically deployed device that will be in water for years. Fast detection of changes in structural health are typically required for environment assessment (i.e., immediate detection of an impact), while more intermittent assessment of structural health can be tolerated with long-term commercial machines. Therefore, for short duration environmental assessment continuous max sampling should be used, providing a sample rate of 500 samples/sec. A 1000 mA-hr battery would last at most around 4 days at this rate. For a two-year deployment of a commercial system with a 1000 mA-hr battery, the transmission system should be operated with at least a duty cycle of 368 to provide a data sample about every 59 seconds.

IV. CONCLUSIONS

The data transmission system can successfully communicate representative structural health data in a benchtop setting and also from the rotating reference frame of a prototype hydrokinetic energy system. Data can be transmitted acoustically underwater from an isolated source (transmitter, blade reference frame) to a static relay station (receiver, fixed reference frame), and then broadcast wirelessly to a remote monitoring station (via Bluetooth). Error in the electronics measuring the structural health signal limits the accuracy of the measurements to ±5%. Results from testing on a prototype hydrokinetic machine indicate that the ultrasonic and Bluetooth communication can transmit 10 bit data with an error fraction of only 0.9% when the acoustic signal is properly guided from the transmitter to receiver. If the acoustic signal is allowed to expand using the current acoustic transducers and signal power level, the data error fraction increases to 2%.

The maximum rate at which the structural health data can be transmitted is 500 samples/sec. Each sample of structural health data is captured by the measurement electronics with 10 bit resolution, and the entire 10 bit data packet is transmitted. With our modified on-off keying encoding scheme, the underwater acoustic communication system must transmit a total of 16 bits: 10 data bits, 4 clock train bits, and 2 termination bits. With the 40 kHz acoustic frequency, each bit requires 0.125 ms, resulting in a total transmission time for 1 data sample of 2 ms. Thus, assuming continuous data transmission, a maximum rate of 500 samples per second can be achieved by the data transmission system.

The optimum mode of operation of the data transmission system is dependent on the hydrokinetic machine application. For prototype testing the data transmission system should operate at maximum sampling rate. Based on our analysis, max sampling rate could be achieved for 50+ hours of testing with any of the battery power sources described. This could include detailed strain response of the system over time, the response to impact or other transient events, and monitoring the evolution of the degradation and damage the blades experience in 'real-time'. A commercially-deployed hydrokinetic system requires a longer lifetime than a prototype system. In this case, the data transmission system should make periodic structural health measurements, transmit the data, and then enter sleep mode to conserve power. Using a relatively low capacity 560 mA-hr battery would provide enough energy to measure the structural health data every 13 minutes 33 seconds throughout a 2 year period. If higher sampling rate is desired, a 1000 mA-hr battery could be used and would enable acquisition and transmission of data every 59 seconds for 2 yrs. Based on the capacity of the battery and duty cycle (sleep vs. awake time) of the system, intermittent monitoring can be achieved for relatively long periods of time.

ACKNOWLEDGEMENTS

The authors wish to thank the Office of Naval Research (grant N00014-10-1-0923) and Department of Energy (grant DE-EE0004569) for supporting this work.

REFERENCES

[1] Khan, M. J., Bhuyan, G., Iqbal, M. T., Quaicoe, J. E., "Hydrokinetic energy conversion systems and assessment of horizontal and vertical axis turbines for river and tidal applications: A technology status review," Applied Energy, Vol. 86, pp. 1823-1835, 2009.

[2] Khan, M. J., Iqbal, M. T., Quaicoe, J. E., "River current energy conversion systems: Progress, prospects and challenges," Renewable and Sustainable Energy Reviews, Vol. 12, pp. 2177-2193, 2008.

[3] Previsic, M., "System Level Design, Performance, Cost and Economic Assessment - Alaska River In-Stream Power Plants," EPRI RP 006 Alaska Electric Power Research Institute, Oct. 31, 2008.

[4] "Hydrokinetic Electric Power Generation," Climate TechBook, Pew Center on Global Climate Change, Dec. 2009.

[5] Walford, C. A., "Wind Turbine Reliability: Understanding and Minimizing Wind Turbine Operation and Maintenance Costs," Sandia Report SAND2006-1100, Prepared by Global Energy Concepts, LLC, Mar. 2006.

[6] "Report to Congress on the Potential Environmental Effects of Marine and Hydrokinetic Energy Technologies," U.S. Dept. of Energy, Dec. 2009.

[7] Sale, M. J., Cada, G. F., Acker, T. L., Carlson, T., Dauble, D. D., Hall, D. G., "DOE Hydropower Program Biennial Report for FY 2005-2006," ORNL/TM-2006/97, U.S. Dept. of Energy, July 2006.

[8] Cada, G., Ahlgrimm, J., Bahleda, M., Bigford, T., Stavrakas, S. D., Hall, D., Moursund, R., Sale, M., "Potential Impacts of Hydrokinetic and Wave energy Conversion Technologies on Aquatic environments," Fisheries, Vol. 32, No. 4, pp. 174-181, April 2007.

[9] Coutant, C. C., Cada., G. F., "What's the future of instream hydro?," Hydro Review XXIV, Vol. 6, pp. 42-49, 2005.

[10] Dutton, A. G., Blanch, M. J., Vionis, P., Lekou, D., Delft, D. R. V. v., Joosse, P. A., Anastassopoulos, A., Kouroussis, D., Kossivas, T., Philippidis, T. P., Assimakopoulou, T. T., Fernando, G., Doyle, C., Proust, A., "Acoustic Emission Condition Monitoring of Wind Turbine Rotor Blades: Laboratory Certification Testing to Large Scale In-Service Deployment," European Wind Energy Conference - EWEC, Madrid, Spain, 2003.

[11] M.J.Blanch, A.G.Dutton, "Acoustic Emission Monitoring of Field Tests of an operating Wind Turbine," Key Engineering Materials, Vol. 245-246, pp. 475-482, July 2003.

[12] Ciang, C. C., Lee, J.-R., Bang, H.-J., "Structural health monitoring for a wind turbine system: a review of damage detection methods," Measurement Science and Technology, Vol. 19, pp. 122001, 2008.

[13] Akyildiz, I. F., Pompili, D., Melodia, T., "Underwater acoustic sensor networks: research challenges," Ad Hoc Networks, Vol. 3, pp. 257-279, 2005.

[14] Robison, K., Watkins, S. E., Nicholas, J., Chandrashekhara, K., Rovey, J. L., "Instrumented Composite Turbine Blade for Health Monitoring," Paper 8347-93, SPIE Smart Structures and Materials, Non-destructive Evaluation, and Health Monitoring Conference, San Diego, CA, Mar. 11-15, 2012.

[15] Watkins, S. E., Robison, K., Nicholas, J., Taylor, G. A., Chandrashekhara, K., Rovey, J. L., "Damage Assessment of Hydrokinetic Composite Turbine Blades Using Fiber Optic Sensors," SPIE-86942B, SPIE Smart Structures/NDE Conference, San Diego, CA, Mar. 10-14, 2013.

[16] H. C. Pumphrey, L. A. Crum and L. Bjorno, "Underwater sound produced by individual drop impacts and rainfall," JASA, vol 4, no. 4, April 1989.

[17] R. B. Mitsen, "Underwater Noise of Research Vessels: Review and Recommendations," International Council for the Exploration of the Sea, Copenhagen, Denmark, May 1995.

[18] M. A. Ainslie, J. G. McColm, "A simplified formula for viscous and chemical absorption in seawater," J. Acoust. Soc. Am., vol 103, no. 3, March 1998

[19] S. Mukherji, N. Kolekar, A. Banerjee, R. Mishra, "Numerical investigation and evaluation of optimum hydrodynamic performance of a horizontal axis hydrokinetic turbine," J. Renewable Sustainable Energy 3, 063105 (2011).